



This is a repository copy of *The Calculation and Interpretation of Parametric Transfer Functions for Binary Distillation Columns of the Tray Type.*

White Rose Research Online URL for this paper:
<http://eprints.whiterose.ac.uk/76165/>

Monograph:

Edwards, J.B. and Tabrizi, M.H.N. (1982) *The Calculation and Interpretation of Parametric Transfer Functions for Binary Distillation Columns of the Tray Type*. Research Report. ACSE Report 169 . Department of Control Engineering, University of Sheffield, Mappin Street, Sheffield

Reuse

Unless indicated otherwise, fulltext items are protected by copyright with all rights reserved. The copyright exception in section 29 of the Copyright, Designs and Patents Act 1988 allows the making of a single copy solely for the purpose of non-commercial research or private study within the limits of fair dealing. The publisher or other rights-holder may allow further reproduction and re-use of this version - refer to the White Rose Research Online record for this item. Where records identify the publisher as the copyright holder, users can verify any specific terms of use on the publisher's website.

Takedown

If you consider content in White Rose Research Online to be in breach of UK law, please notify us by emailing eprints@whiterose.ac.uk including the URL of the record and the reason for the withdrawal request.



eprints@whiterose.ac.uk
<https://eprints.whiterose.ac.uk/>

629.8 (S)

THE CALCULATION AND INTERPRETATION OF PARAMETRIC TRANSFER FUNCTIONS
FOR BINARY DISTILLATION COLUMNS OF THE TRAY TYPE

BY

J.B. Edwards^{*} and M.H.N. Tabrizi[†]

A revised paper submitted to the Institution of Chemical Engineers
for consideration for publication in the Transactions

February 1982

Research Report No. 169

* Senior Lecturer, Department of Control Engineering, University of
Sheffield, Mappin Street, Sheffield S1 3JD.

† Research Student in the same Department.

SYNOPSIS

Starting from familiar assumptions for dynamic analysis, a transfer-function-matrix (T.F.M) model for long, symmetrical, binary distillation columns is derived completely analytically. The model relates twin output composition changes to perturbations in the internal liquid and vapour flow rates. The model is intended for use in controller design and, being expressed in terms of plant parameters and operating conditions, should provide useful common ground between control engineer and plant designer. Though derived precisely for a symmetrical plant, it is expected that the model should apply more generally as a good approximation. Experimental data is given supporting this claim.

Inverse Nyquist loci are generated in precise and approximate form and shown to compare favourably with computed step responses. The responses accord broadly with previous, part empirical, part numerical research results.

The paper is the first of a companion pair, the second being devoted to packed-column analysis.

5 069388 01



1. List of Symbols

α	- initial slope of equilibrium curve approximation
ϵ	- $\alpha-1$
F	- molar feed rates of liquid and vapour
G	- normalised spatial composition gradient in steady-state
\underline{G}	- transfer function matrix (T.F.M.)
$\frac{G}{-A}$	- approximation T.F.M.
g_{11}, g_{22}	- diagonal elements of \underline{G}
g_{A11}, g_{A22}	- diagonal elements of $\frac{G}{-A}$
H_{ℓ}, H_{ℓ}'	- liquid capacitances p.u. length of rectifier and stripper
H_a, H_b	- capacitances of accumulator and reboiler
h'	- distance along column measured from top and bottom
δh	- tray spacing
h	- normalised distance ($h'/\delta h$)
\underline{I}	- unit diagonal 2x2 matrix
L	- normalised lengths of rectifier and stripper
L_r, L_s, ℓ	- molar flows of liquid in rectifier and stripper and small changes therein
p	- Laplace variable for transforms w.r.t. τ
\underline{q}	- vector of difference and total of vapour and liquid composition changes
s	- Laplace variable for transforms w.r.t. h
t	- time
τ	- normalised time ($=tV_r/\alpha H_{\ell} \delta h'$)
T_a, T_b	- normalised time-constants of accumulator and reboiler (= T where identical)
\underline{u}	- vector of total and difference in vapour and reflux rate changes

- $V_r (=V), V_s, v$ - molar flows of vapour in rectifier and stripper and small changes therein
- X, X' - liquid compositions (mol fractions) in rectifier and stripper
- x, x' - small changes in X and X'
- Y, Y' - vapour compositions in rectifier and stripper
- y, y' - small changes in Y and Y'
- Z - feed liquid composition
- z - feed vapour composition
- $\tilde{}$ - superscript denoting Laplace transforms w.r.t. h and τ
- \sim - superscript denoting Laplace transforms w.r.t. τ only
- T.F.M. - transfer-function matrix
- p.d.e. - partial differential equation
- d.e. - ordinary differential equation

2. Introduction

The accurate calculation^{*} of transfer-function matrices (T.F.M.'s) for the composition dynamics of columns, by completely analytical methods, has not been achieved hitherto despite several decades of column research worldwide. Transfer-functions have been obtained either entirely experimentally or part-analytically, incorporating approximation or empirical data to overcome difficult steps in the analysis. As a result, the range of application of existing T.F.M. models to varying plants and operating conditions remains limited. It is common experience that different columns differ enormously, yet inexplicably, in their behaviour, especially if trials are allowed to run for the full settling-time.

The difficulties arise from the complexity of the expressions which develops quite early in the analysis of even the simplest hypothetical system. This comes about partly from nonlinearity and the spatial distribution of the variables, but more importantly, from the two-stage construction of columns and the associated boundary conditions. To simplify the equations, the analyst usually begins to neglect apparently small terms but this can be disastrous because their effects cannot be properly judged a priori since column dynamics are driven by small differences in large terms. Other, late, approximations may involve lumping of spatial variables and relaxation of boundary conditions (assuming these were correctly formulated in the first place). Predictions are sometimes tested against experiment but, whereas reasonable agreement has been achieved in trials on one-off plants, it can be difficult to tell whether success is due to the quality of the analysis or the incorporation of empirical data derived often from the same, or similar plant to that used for final model validation.

* We stress the distinction between (a) the accurate calculation of T.F.M.'s and (b) the calculation of accurate T.F.M.'s. The authors believe that in attempting (b), by reducing initial approximation, results may be obtained that are inferior (through enforced approximation later on in the calculation) to those achievable by simplifying initially and thence proceeding accurately, i.e. as (a).

Irrespective of the quality of existing transfer-function models, however, the case for seeking parametric T.F.M's by pure analysis remains very strong, since few would argue that the full range of parameter space has been comprehensively explored. One of the authors' initial motivations for the analytical research at Sheffield was the failure of an existing, apparently general, model to predict the separation/vapour-rate relationship observed on a pilot column installed there. This point is considered in the companion⁽¹⁾ to the present paper. The case for analytical study is enhanced by the fact that the rival approach, viz computer simulation, is expensive and fraught with numerical accuracy and stability problems where column equations are concerned.

One important purpose of a parametric T.F.M. is, (a), to provide a useful test of an initially doubtful simulation before using this on a large programme of experiments. Another is, (b), that of providing a basis for control system design, or, (c), of validating a grossly simplified T.F.M., itself to be used for controller design. A fourth purpose, (d), is to indicate, simply by inspection of the T.F.M. formulae, the broad effect, i.e. the approximate trend, on behaviour of plant-parameter change, noting that in a linearised model of a nonlinear process such as this, the term plant-parameter embraces quiescent operating conditions. This allows useful dialogue between plant-designer and control-system engineer.

For all these purposes, (a) - (d), a parametric model based on primary effects alone should be adequate, particularly where no such model existed previously. In this paper (and a companion devoted to packed columns) the authors derive and examine T.F.M's describing the main thermodynamically-driven, mass-transfer effects alone, i.e. those relationships which make the column distill, rather than the secondary effects, such as hydrodynamics, heat-loss etc., which cause its behaviour to deviate from the ideal. We make idealising assumptions entirely at the outset and then proceed without

further approximation. This is in important contrast with most previous work where many secondary relationships are included initially (for the sake of apparent generality and practicality) but where subsequent approximation is made as the mathematical difficulties increase. In Section 3 we consider our initial approximations (or, preferably-idealizations) which we believe to be no more restrictive than those used to introduce steady-state distillation in text books⁽²⁾. Indeed we believe such simplifications to be illuminating rather than confusing and particularly justified in dynamic column analysis which is still in its infancy when compared to steady-state analysis.

3. System Equations and Idealizations

3.1 Equilibrium assumptions

We approximate the mixture's equilibrium curve by two straight lines shown in Fig. 1, these being

$$(1 - X) = \alpha(1 - Y_e) \quad , \text{ rectifier} \quad (1)$$

$$\text{and} \quad Y' = \alpha X_e' \quad , \text{ stripping section} \quad (2)$$

where, for the lighter component, Y_e is the equilibrium/mol-fraction associated with a liquid of mol-fraction X in the rectifier, whilst X_e' is the equilibrium liquid mol-fraction associated with a vapour of mol-fraction Y' in the stripping section. The constant slope parameter α (> 1.0) is related to the relative volatility and the symmetry of the relationship about the -45° line in Fig. 1, like that of an ideal mixture's true equilibrium curve, is noteworthy. Piecewise linearisation in this manner has often been used in dynamic analyses attempted in the past and notably in the pioneering studies of Wilkinson and Armstrong^{(2)*} and by others. In tray columns it is usually assumed that theoretical trays operate in equilibrium so that

* Wilkinson and Armstrong's work was, however, directed at the analytical determination of time-domain responses, necessitating considerable approximation in the later stages.

$$Y(h;t) = Y_e(h',t) \quad (3)$$

and $X(h;t) = X_e(h',t) \quad (4)$

where Y and X' are the actual mol-fractions of vapour and liquid in the rectifier and stripping sections at points distant h' from the top and bottom of the tower respectively. As in introductory texts⁽²⁾ on steady-state design, each tray is here taken to be an ideal, or theoretical, tray. Non-ideal behaviour from the non-attainment of equilibrium can have important dynamic results that are examined in the companion paper⁽¹⁾.

3.2 Heat-and mass-balances

The main column variables and parameters are indicated in Fig. 2. As regards heat balance, we neglect sensible heat changes, mechanical work associated with vapour compression and all heat loss from the plant other than via the condenser and outflows. This is again in accord with introductory steady-state analyses designed to yield insight rather than to generate detail. We are therefore left with only latent heat transfer and, if the two components have equal latent heats per mol, the overall rates of evaporation and condensation on any given tray will always balance so that the vapour and liquid flow rates V_r, V_s, L_r and L_s will be independent of h' and depend on time t only. (Fictitious molecular weights may be introduced to accommodate unequal latent heats if necessary as Stainthorp⁽⁴⁾ has pointed out). This independence of flow-rate and h' is the so called constant-molar-overflow assumption used in many previous investigations^{(5), (6), (7), (8), (9),} along with the linearised equilibrium curve assumption.

As is usual in tray column modelling we here regard vapour capacitance as being negligible in comparison to the molar liquid capacitances $H'_l \delta h$ and $H_l \delta h$ of each rectifier and stripping section tray. Taking mass balances on the lighter component on a typical tray in the rectifier therefore yields a simple differential equation involving finite differences w.r.t h' to which Taylor's theorem may be applied assuming a large number of trays at

small spacing δh . This operation together with the use of equations (1) and (3) to eliminate $X(h',t)$ in favour of $Y(h',t)$ gives the partial differential equation (p.d.e):

$$\alpha \frac{\partial (H_\ell Y)}{\partial t} \delta h = -(\alpha L_r - V_r) \frac{\partial Y}{\partial h'} \delta h + \frac{1}{2} (\alpha L_r + V_r) \frac{\partial^2 Y}{(\partial h')^2} (\delta h)^2 \quad (5)$$

whilst for the stripping section we deduce:

$$\frac{\partial (H'_s X')}{\partial t} \delta h = (L_s - \alpha V_s) \frac{\partial X'}{\partial h'} \delta h + \frac{1}{2} (L_s + \alpha V_s) \frac{\partial^2 X'}{(\partial h')^2} (\delta h)^2 \quad (6)$$

The Taylor expansions have been taken to second powers of δh only on the assumption that we are dealing with many trays in total, i.e. long columns. The criteria for a so-called long column will be investigated in Section 5.

3.3 Linearisation for small perturbations

As p.d.e's (5) and (6) are nonlinear (the flows being variable controls), linearisation is essential at the outset if T.F.M's are to be derived. If we confine attention to linearisation about the steady-state, i.e. about the condition $\partial Y/\partial t = \partial X'/\partial t = 0$, then, irrespective of hydrodynamics* causing variations in H_ℓ and H'_s , on implicit differentiation of (5) and (6) we obtain the following p.d.e's relating small variations y and x' in Y and X' to small perturbations v and ℓ in the circulating vapour and liquid flow-rates, viz:

$$\begin{aligned} \alpha H_\ell \frac{\partial y}{\partial t} \delta h = & -(\alpha L_r - V_r) \frac{\partial y}{\partial h'} \delta h + \frac{1}{2} (\alpha L_r + V_r) \frac{\partial^2 y}{(\partial h')^2} (\delta h)^2 \\ & - \frac{\partial Y}{\partial h'} \delta h (\alpha \ell - v) + \frac{1}{2} \frac{\partial^2 Y}{(\partial h')^2} (\delta h)^2 (\alpha \ell + v) \end{aligned} \quad (7)$$

$$\begin{aligned} H'_s \frac{\partial x'}{\partial t} \delta h = & (L_s - \alpha V_s) \frac{\partial x'}{\partial h'} \delta h + \frac{1}{2} (L_s + \alpha V_s) \frac{\partial^2 x'}{(\partial h')^2} (\delta h)^2 \\ & + \frac{\partial X'}{\partial h'} \delta h (\ell - \alpha v) + \frac{1}{2} \frac{\partial^2 X'}{(\partial h')^2} (\delta h)^2 (\ell + \alpha v) \end{aligned} \quad (8)$$

Provided v and ℓ are kept sufficiently small, steady-state values may be substituted for all the variables in (7) and (8) represented by capital symbols thus yielding linear relationships between y, x' and v, ℓ .

* Hydrodynamics have in any event been shown by Armstrong and Wood⁽¹²⁾ be basically a cascade process essentially decoupled from the composition dynamics which may therefore be separately analysed.

3.4 Choice of operating conditions and plant parameters

Solution of p.d.e's (7) and (8) is eased considerably if they and the boundary conditions (yet to be derived) are rendered symmetrical by appropriate choice of plant parameters and quiescent operating conditions. Choosing equal lengths, L' and equal tray spacings, δh for the rectifier and stripping section are the first obvious steps towards symmetry as is setting

$$\alpha H_{\ell} = H'_{\ell} \quad (\stackrel{\Delta}{=} H) \quad (9)$$

A symmetrical equilibrium curve approximation has already been assumed (equations 1 and 2).

Inspection of the steady-state large-signal equations, obtained by setting $\partial/\partial t = 0$ in (5) and (6) reveals that by operating at

$$\alpha L_r = V_r \quad \text{and} \quad \alpha V_s = L_s \quad (10)$$

then steady state compositions are governed by

$$\partial^2 Y / (\partial h')^2 = \partial^2 X' / (\partial h')^2 = 0 \quad (11)$$

so that the quiescent composition gradients are constant, giving uniform loading throughout each section. Equal tray loadings throughout the entire column is clearly the best practical operating condition (in view of equation 9) and, for this, further symmetry is needed as the steady-state solution, given in Section 3.7, reveals. The required conditions for

$$- \partial Y / \partial h' = \partial X' / \partial h' = G = \text{constant} > 0 \quad (12)^*$$

are
$$V_r = L_s \quad (\stackrel{\Delta}{=} V) \quad , \quad V_s = L_r \quad (13)$$

and equal proportion of liquid and vapour in the feed so that

$$F_v = F_{\ell} \quad (\stackrel{\Delta}{=} F) \quad (14)$$

yielding equal output rates, $V_r - L_r$ and $L_s - V_s = F$ at top and bottom. Finally to avoid pinch effects at the feedpoint the feed mixture should be in equilibrium as regards both sections, i.e. its vapour and liquid

* The - ve sign indicates that Y increases as h' reduces as expected since h' is measured from the top of the rectifier downwards towards the feed.

compositions y and z should reside at the knee of Fig. 1 so that

$$z = \frac{\alpha}{1+\alpha} \quad \text{and} \quad Z = \frac{1}{1+\alpha} \quad (15)$$

Solution is thus confined to a range of special cases but this should not be regarded as unduly restrictive because, in many respects, this is a range of ideals for which practical design should strive. The even tray-loading condition is but one attribute of this special case range, and is a condition which has often been assumed explicitly or implicitly in column studies (5), (6), (7), (8), (9), both dynamic and steady-state. Other attributes will become clear when the steady-state solution is considered in more detail.

3.5 Normalisation

Inserting the foregoing operating conditions in p.d.e's (7) and (8) and normalising by setting

$$h = h'/\delta h \quad , \quad \tau = t/T_n \quad (16)$$

where base time T_n is the time for liquid to travel base-distance δh

$$\text{i.e.} \quad T_n = \alpha H_\ell \delta h / V = H_\ell \delta h / L_r \quad (17)$$

we obtain the greatly simplified forms

$$\partial y / \partial \tau = \partial^2 y / \partial h'^2 - (G/V)(v - \alpha \ell) \quad (18)$$

$$\text{and} \quad \partial x' / \partial \tau = \partial^2 x' / \partial h'^2 + (G/V)(\ell - \alpha v) \quad (19)$$

Their solution of course requires not only knowledge of inputs $v(\tau)$ and $\ell(\tau)$ but also steady-state composition gradient G (see Section 3.7) and the process boundary condition considered next.

3.6 Boundary conditions (large-signal)

3.6.1 Accumulator and reboiler Denoting accumulator and reboiler mol-fractions by $Y(o)$, $X(o)$ and $Y'(o)$, $X'(o)$ respectively and taking mass balances on these vessels yields

$$\frac{\partial \{H_a X(o)\}}{\partial t} = V_r \{Y(\delta h) - X(o)\} = V_r \left\{ Y(o) + \frac{\partial Y}{\partial h'} \bigg|_{h'=0} \delta h - X(o) \right\}$$

$$\text{or, writing } \varepsilon = \alpha - 1 \quad (20)$$

$$\alpha \frac{\partial \{H_a Y(o)\}}{\partial t} = V_r \left\{ \varepsilon - \varepsilon Y(o) + \frac{\partial Y}{\partial h'} \bigg|_{h'=0} \delta h \right\} \quad (21)$$

which, after normalising becomes

$$\frac{\partial \{T_a Y(o)\}}{\partial \tau} = \varepsilon \{1 - Y(o)\} + \left. \frac{\partial Y}{\partial h} \right|_{h=0} \quad (22)$$

and

$$\begin{aligned} \frac{\partial \{H_b X'(o)\}}{\partial t} &= L_s \{X'(\delta h) - Y'(o)\} = L_s \{X'(o) + \left. \frac{\partial X'}{\partial h'} \right|_{h'=0} \delta h - Y'(o)\} \\ &= L_s \left\{ -X'(o) \varepsilon + \left. \frac{\partial X'}{\partial h'} \right|_{h'=0} \delta h \right\} \end{aligned} \quad (23)$$

which normalises to give

$$\frac{\partial \{T_b X'(o)\}}{\partial \tau} = -\varepsilon X'(o) + \left. \frac{\partial X'}{\partial h} \right|_{h=0} \quad (24)$$

where $T_a = H_a/H_l \delta h$ and $T_b = H_b/H \delta h$ (25)

H_a and H_b being the molar capacitances of the accumulator and reboiler. The R.H. terms in equations (21) and (23) have been obtained by applying first-order Taylor expansions to the finite differences $Y(\delta h) - Y(o)$ and $X'(\delta h) - X'(o)$ which is valid for a sufficiently small δh .

3.6.2 Feed-trays A mass balance on the rectifier feed tray yields

$$\begin{aligned} \frac{\partial H_l X(L)}{\partial t} \delta h &= F z + V_s Y'(L) - V_r Y(L) + L_r \{X(L - \delta h) - X(L)\} \\ &= F z + V_s Y'(L) - V_r Y(L) - L_r \left. \frac{\partial X}{\partial h'} \right|_{h'=L'} \delta h \end{aligned} \quad (26)$$

on applying a first-order Taylor expansion. Now from symmetry conditions (10), (13) and (14) we deduce that

$$F = \varepsilon V \quad (27)$$

so that substituting for F and z in (25) gives, after normalisation

$$\frac{\partial Y(L)}{\partial \tau} = -\frac{2}{\alpha+1} + X'(L) + \{1 - Y(L)\} - \left. \frac{\partial Y}{\partial h} \right|_{h=L} \quad (28)$$

and, similar treatment of the stripping section's feed tray yields

$$\frac{\partial X'(L)}{\partial \tau} = \frac{2}{\alpha+1} - X'(L) - \{1 - Y(L)\} + \left. \frac{\partial X'}{\partial h} \right|_{h=L} \quad (29)$$

The symmetry of (22) and (25) and of (27) and (28) is noteworthy.

3.7 Large-signal steady-state solution: justifying symmetry

Having formed the large signal boundary conditions, (22), (24), (28) and (29) and setting $\partial/\partial\tau = 0$, the large signal steady state-equations (11) for our symmetrical plant may be readily solved to produce the linear solution for $Y(h)$ and $X'(h)$ graphed in Fig. 3. from which we note in particular the constant value of slope G , i.e.

$$G = 2 \epsilon / \{ (\alpha+1) (2\epsilon L + \alpha + 1) \} \quad (30)$$

and the fact that

$$X'(h) = 1 - Y(h) \quad (31)$$

The results are necessary for substitution in the solution to our linearised small-signal model (18) and (19) but have a strong practical appeal in themselves. The constancy of G , leading to even tray loading, has already been anticipated and discussed but equation (30) represents another important attribute of the special case we have adopted. The result indicates that, having started from a 50/50 mixture of components ($z + Z = 0.5$) i.e. as disordered a feed mixture as possible, the choice of a symmetrical plant and operating regime has produced top and bottom products that are equally pure, nominally, in terms of light and heavy component respectively. Now in a truly twin product control problem, both product purities will ideally have equal priority, and any shift in importance from one to the other represents a shift from a 2x2 to a single-input, single-output problem i.e. a simpler problem. Control, in its widest sense, is achieved (a) by plant design initially and (b) by automatic regulation thereafter and we have so-far ensured that stage (a) yields products nominally in accord with the ideal 2-input, 2-output control problem. In cases where the feed composition were richer (weaker) then, to avoid pinch effects, this would be entered nearer to the accumulator (reboiler) so approaching a single-stage situation, capable of easier analysis⁽¹²⁾. We believe therefore that in considering a symmetrical plant, we are investigating the most thoroughly 2-input, 2-output, 2-stage process. This need not

restrict the validity of the resulting T.F.M., or indeed the steady-state solution above, to precisely symmetrical processes for, hopefully, the results will be sufficiently robust to apply, as good approximations, in the presence of considerable deviations from symmetry. The stretching of the region of validity is really no different philosophically to the extension of linearised models from infinitesimal, to moderate perturbations: a universal practice in control and process engineering.

As a final justification for proceeding with the symmetrical case, we would emphasise that static symmetry has often been assumed by previous researchers, but implicitly rather than explicitly. Shinskey's empirical relationship⁽¹⁰⁾ between separation and vapour rate, for instance, approaches mathematical accuracy most nearly for symmetrical systems. Rosenbrock's simulation observations⁽⁷⁾, confirmed by McMorran's frequency-domain studies⁽¹¹⁾, relating composition-tilt to vapour-rate and average composition to distillate-rate are again most apt in the symmetrical case. Nearly equal composition gradients are a frequent feature of approximate analysis whereas in other cases, e.g. Armstrong and Wood⁽¹²⁾ interaction between the two stages has been neglected by artificially fixing the feed tray composition.

3.8 Small signal boundary conditions

These are derived from the large signal boundary equations (21), (23) (26) (and a similar equation for the stripper feed tray) and the assumed (symmetrical) operating conditions. For the accumulator for instance we get, on implicit differentiation:

$$\alpha_H \frac{\partial y(o)}{\partial t} = v \left\{ -y(o)\epsilon + \epsilon + \frac{\partial y}{\partial h} \right\} \Big|_{h'=0} \delta h + v_r \left\{ -\epsilon y(o) + \frac{\partial y}{\partial h} \right\} \Big|_{h'=0} \delta h$$

the first-term of the R.H.S. being zero in steady state so that normalising we get simply

$$T_a \frac{\partial y(o)}{\partial \tau} = -\epsilon y(o) + \frac{\partial y}{\partial h} \Big|_{h=0} \quad (32)$$

whilst for the stripping section we obtain

$$T_b \frac{\partial x'(0)}{\partial \tau} = -\epsilon x'(0) + \left. \frac{\partial x'}{\partial h} \right|_{h=0} \quad (33)$$

For the feed tray, from (26) we get

$$H_\ell \delta h \frac{\partial x(L)}{\partial \tau} = v\{Y'(L) - Y(L)\} + \ell \alpha G + V_s Y'(L) - V_r Y(L) - L_r \left. \frac{\partial x}{\partial h} \right|_{h=L'} \delta h \quad (34)$$

From the steady state solution we find that

$$Y'(L) - Y(L) = -G(\alpha+1)/2 \quad (35)$$

and hence the rectifier feed condition is:

$$\frac{\partial y(L)}{\partial \tau} = \frac{G}{V_r} \left\{ -\frac{(\alpha+1)}{2} v + \alpha \ell \right\} - \left. \frac{\partial y}{\partial h} \right|_{h=L} + x'(L) - y(L) \quad (36)$$

and by similar means we deduce the stripper feed equation to be:

$$\frac{\partial x'(L)}{\partial \tau} = \frac{G}{V_r} \left\{ -\alpha v + \frac{(\alpha+1)}{2} \ell \right\} - \left. \frac{\partial x'}{\partial h} \right|_{h=L} + y(L) - x'(L) \quad (37)$$

4. Solving for the T.F.M.

The small signal behaviour of the symmetrical column compositions, given the flow disturbances $v(t)$, $\ell(t)$ is now completely specified by p.d.e.'s (18) and (19) and boundary conditions (32), (33), (36) and (37), the symmetry of which, with our chosen outputs y and x' , is striking. This leads to the ready diagonalisation of the system if we adopt the following output and input vectors, viz

$$\underline{q}(h) = \begin{pmatrix} y(h, \tau) - x'(h, \tau) \\ y(h, \tau) + x'(h, \tau) \end{pmatrix} \quad (38) \quad \text{and} \quad \underline{u}(\tau) = \frac{G}{V} \begin{pmatrix} v(\tau) + \ell(\tau) \\ v(\tau) - \ell(\tau) \end{pmatrix} \quad (39)$$

Laplace transforming (18) and (19) in s w.r.t. h and in p w.r.t. τ and adding and subtracting the resulting equations gives

$$(s^2 - p) \tilde{\underline{q}} - s \tilde{\underline{q}}(0) - \tilde{\underline{q}}(0) = s^{-1} \begin{pmatrix} -\epsilon & 0 \\ 0 & \alpha+1 \end{pmatrix} \tilde{\underline{u}} \quad (40)$$

where $\tilde{\underline{q}}(s, p)$ is the double transform of $\underline{q}(h, \tau)$, $\tilde{\underline{q}}(0)$ is the transform of

$\underline{q}(0, \tau)$: w.r.t τ , \tilde{u} that of $u(\tau)$ and $\tilde{\underline{q}}(0)$ that of $\partial q / \partial h$ at $h = 0$. The end vessel conditions (32) and (33) yield, if $T_a = T_b = T$,

$$T p \tilde{\underline{q}}(0) = -\epsilon \tilde{\underline{q}}(0) + \tilde{\underline{q}}(0) \quad (41)$$

so that eliminating $\tilde{\underline{q}}(0)$ gives

$$(s^2 - p) \tilde{\underline{q}} - (s + \epsilon - Tp) \tilde{\underline{q}}(0) + s^{-1} \begin{pmatrix} \epsilon & 0 \\ 0 & -(\alpha+1) \end{pmatrix} \tilde{\underline{u}} = 0 \quad (42)$$

and inversion back to the h, p domain, and setting $h = L$ therefore yields

$$\tilde{\underline{q}}(L) - \underline{Q}_1(L) \tilde{\underline{q}}(0) - \underline{Q}_2(L) \tilde{\underline{u}} = 0 \quad (43)$$

where $\underline{Q}_1(h) = (\mathcal{L} T_h)^{-1} \{(s + \epsilon + Tp) / (s^2 - p)\} \underline{I}$

$$= \{\sqrt{p} \cosh \sqrt{p} L + (\epsilon + Tp) \sinh \sqrt{p} L\} \underline{I} / \sqrt{p} \quad (44)$$

and

$$\begin{aligned} \underline{Q}_2(h) &= (\mathcal{L} T_h)^{-1} \left\{ \frac{1}{s(s^2 - p)} \begin{pmatrix} -\epsilon & 0 \\ 0 & \alpha+1 \end{pmatrix} \right\} \\ &= \frac{\cosh \sqrt{p} L - 1}{p} \begin{pmatrix} -\epsilon & 0 \\ 0 & \alpha+1 \end{pmatrix} \end{aligned} \quad (45)$$

where \underline{I} is a 2x2 unit diagonal matrix. Now the feed boundary conditions for $\underline{q}(L)$, i.e. equations (36) and (37) may be expressed thus:

$$\underline{Q}_3 \tilde{\underline{q}}(L) + \frac{\partial}{\partial h} \tilde{\underline{q}}(h) \Big|_{h=L} = \underline{Q}_4 \tilde{\underline{u}} \quad (46)$$

$$\text{where } \underline{Q}_3 = \begin{pmatrix} p+2 & , & 0 \\ 0 & , & p \end{pmatrix} \text{ and } \underline{Q}_4 = \begin{pmatrix} 0.5\epsilon & & 0 \\ 0 & & -0.5(3\alpha+1) \end{pmatrix} \quad (47)$$

allowing unknown $\tilde{\underline{q}}(L)$ to be eliminated between (43) and (46) giving

$$\tilde{\underline{q}}(0) = \underline{G}(0, p) \tilde{\underline{u}} \quad (48)$$

where T.F.M. $\underline{G}(0, p)$ relating end compositionsto flow rates is given by:

$$\underline{G}(0, p) = \left(\underline{Q}_3 \underline{Q}_1 + \frac{\partial \underline{Q}_1}{\partial h} \right)^{-1} \left(\underline{Q}_4 - \underline{Q}_3 \underline{Q}_2 - \frac{\partial \underline{Q}_2}{\partial h} \right) \Big|_{h=L} \quad (49)$$

Since all the matrices on the R.H.S. of (49) are diagonal, $\underline{G}(0, p)$ takes the diagonal form

$$\underline{G}(o,p) = \begin{pmatrix} g_{11}(o,p) & 0 \\ 0 & g_{22}(o,p) \end{pmatrix} \quad (50)$$

and from the known expressions for $Q_1 \dots Q_4$ we quickly obtain the individual transfer functions

$$g_{11}(o,p) = \frac{\varepsilon\{(p+2)(\cosh\sqrt{p}L - 1)/p + (\sinh\sqrt{p}L)/\sqrt{p} + 0.5\}}{\{(1+T)p + 2 + \varepsilon\}\cosh\sqrt{p}L + \{(p+2)(\varepsilon + T_p) + p\}(\sinh\sqrt{p}L)/\sqrt{p}} \quad (51)$$

and

$$g_{22}(o,p) = - \frac{(\alpha+1)(\cosh\sqrt{p}L - 1) + (\alpha+1)(\sinh\sqrt{p}L)/\sqrt{p} + 0.5(3\alpha+1)}{\{p(1+T) + \varepsilon\}\cosh\sqrt{p}L + \sqrt{p}(1 + \varepsilon + T_p)\sinh\sqrt{p}L} \quad (52)$$

the limiting values for $p = 0$ being:

$$g_{11}(o,0) = \varepsilon(L^2 + L + 0.5)/(2\varepsilon L + \alpha + 1) \quad (53)$$

and

$$g_{22}(o,0) = - \{(\alpha+1)L + 0.5(3\alpha + 1)\}/\varepsilon \quad (54)$$

5. Behaviour Predictions

A completely analytic T.F.M. model relating the behaviour of $y(o,\tau)$, $x'(o,\tau)$ to $v(\tau)$, $\ell(\tau)$ has thus been derived in terms of normalised complex frequency p and normalised column length L , both readily converted to real frequency p' and real length L' by the formulae

$$p' = p L_r / (H_\ell \delta h) \quad (55)$$

$$\text{and } L' = L \delta h \quad (56)$$

The real time constant T' of the end vessels is obtainable from its normalised value thus:

$$T' = T H_\ell \delta h / L_r = H_a / L_r = H_b / L_r \quad (57)$$

In terms of y, x, v and ℓ , the model may be expressed:

$$\begin{pmatrix} \tilde{y}(o,p) - \tilde{x}'(o,p) \\ \tilde{y}(o,p) + \tilde{x}'(o,p) \end{pmatrix} = G V_r^{-1} \begin{pmatrix} g_{11}(o,p) & 0 \\ 0 & g_{22}(o,p) \end{pmatrix} \begin{pmatrix} \tilde{v}(p) - \tilde{\ell}(p) \\ \tilde{v}(p) - \tilde{\ell}(p) \end{pmatrix} \quad (55)$$

where G is the steady-state composition gradient readily obtained from α and L via (30). Certain deductions concerning the systems' dynamic

behaviour are immediately obvious from this model whilst others require a deeper examination of the formulae for g_{11} and g_{22} . Of the former, we note that, over the entire frequency range, composition-tilt, $y(h,\tau) - x'(h,\tau)$ is driven noninteractively by average circulating flow $\{v(\tau) + \ell(\tau)\}/2$ whilst composition-total $y(h,\tau) + x'(h,\tau)$ is driven purely by take-off rate $v(\tau) - \ell(\tau)$. We note also that the tilt gain $g_{11}(0,0)$ is positive whilst $g_{22}(0,0)$ is negative and that for low- ϵ relative volatility mixtures ($\epsilon \ll 1.0$) requiring long columns ($L \gg 1.0$ - see steady state solution), then $|g_{11}(0,0)| \ll |g_{22}(0,0)|$.

These findings accord well with say, Rosenbrock's simulation experience⁽⁷⁾ Rademaker's, deductions⁽¹³⁾ and Shinskey's empirical data⁽¹⁰⁾. They, however, reported that separation is influenced predominantly by $v(\tau)$. The conclusions are clearly in close accordance, particularly for the low-relative volatility case where large reflux ratios are needed so allowing $|(v + \ell)| \gg |v - \ell|$.

5.1 Inverse Nyquist Loci

Typical loci of $g_{11}^{-1}(0, j\omega)$ and $g_{22}^{-1}(0, j\omega)$ computed from (51) and (52) are illustrated in Figs. 4 and 5 for $\alpha = 1.1$ ($\epsilon = 0.1$), $L = 10$, $T = 1.0$ (corresponding to a separation $2 GL = 0.46$). Their substantially vertical nature over a wide range of ω , indicating a substantially exponential step response as confirmed by the simulation results of Figs. 6 and 7. Their steady state gains (≈ 2.6 and -225.0) and time constants (≈ 25 and 140) accord closely with those predicted by the loci (i.e. gains of 0.37^{-1} and -0.0048^{-1} and time constants of 0.04^{-1} and 0.0077^{-1}).

The straight vertical nature of the loci, and hence the broadly first-order lag nature of the responses, may be deduced analytically from (51) and (52) however, without recourse to precise computation, by examination of the expressions for g_{11} and g_{22} at large p : Considering the band

$$1.0 \gg |p^{0.5}| \gg 1/L \quad (56)$$

which is a wide band for long columns, it is clear that $\cosh\sqrt{p}L$ and $\sinh\sqrt{p}L \rightarrow 0.5 \exp(\sqrt{p}L)$, ($\gg 1.0$), since

$$\sqrt{p} = (0.5\omega)^{0.5} (1 + j) \quad , \quad p = j\omega \quad (57)$$

Because of the upper bound on p set by (56), only the lowest powers of p outside the hyperbolic functions need be retained so that

$$g_{11}(0,p) \rightarrow \epsilon \{2/p + 1/\sqrt{p}\} / \{2 + \epsilon + 2\epsilon/\sqrt{p}\} \quad (58)$$

$$\text{and } g_{22}(0,p) = (\alpha+1)(1+1/\sqrt{p}) / \{p(1+T) + \epsilon + \sqrt{p}(1+\epsilon+T_p)\} \quad (59)$$

the exponential terms all cancelling out. Now for mixtures of low relative-volatility, (requiring $L \gg 1.0$ for adequate separation)

$$\epsilon \ll 1.0$$

$$\text{so that } \left. \begin{aligned} g_{11}^{-1}(0,p) &= (1+\alpha)p/2\epsilon \\ \text{and } g_{22}^{-1}(0,p) &= -\alpha p/(1+\alpha) \end{aligned} \right\} L^{-1} \ll |p^{0.5}| \ll 1.0 \quad (60)$$

The system is therefore predicted to tend to an integrating process over a wide range of frequency as observed, though its behaviour does become more complicated at higher frequencies. The band considered is wide however since in the region, $L^{-1} \ll \omega^{0.5} \ll 1.0$

$$|g_{11}^{-1}(0,j\omega)| \approx \omega/\epsilon \text{ and } |g_{22}^{-1}(0,j\omega)| \approx \omega/2 \quad (61)$$

and these values are large compared to the static inverse gains

$$|g_{11}^{-1}(0,0)| \approx 2/L \text{ and } |g_{22}^{-1}(0,0)| \approx \epsilon/2L \quad (62)$$

The near first-order lag nature of the systems responses is thus predicted quantitatively, for any long column without computation. The prediction accords qualitatively with previous experience and approximate analyses. The more complex behaviour predicted at very high ω should not be ignored however.

5.2 Effect of terminal capacitance

It is noteworthy that the parameter T drops out of the high frequency analysis above from which we may predict that only the final portion of the step-resonse is influenced by changes in T . This is indeed confirmed by the simulation result of Fig. 8 for $\epsilon = 0.1$, $L = 10$ with $T = 1, 20$ and 50 .

6. Approximate multivariable first-order lag model

One of the motivations for deriving $\underline{G}(o,p)$ has been to validate simpler models. Because the system is class-0 and tends to an integrating process over a wide frequency range, the multivariable first-order lag approximant, $\underline{G}_A(o,p)$ of Owens⁽¹⁴⁾ would appear to be a suitable candidate where

$$\underline{G}_A^{-1}(o,p) = \underline{A}_1 + \underline{A}_o p \quad (63)$$

$$\underline{A}_1 = \lim_{p \rightarrow 0} \underline{G}_A^{-1}(o,p)$$

and

$$\underline{A}_o = \lim_{|p| \rightarrow \infty} \{p^{-1} \underline{G}_A^{-1}(o,p)\} \quad (64)$$

In our case, however, we should strictly replace $|p| \rightarrow \infty$ by $L^{-1} \ll |p^{0.5}| \ll 1.0$ but the approximant should still apply as a basis for controller design provided excessive gains are avoided. Now \underline{A}_1 and \underline{A}_o are readily derived analytically in this case. \underline{A}_1 merely involves solution of the small-signal spatial differential equations obtained by setting $\partial/\partial\tau = 0$ in (18) and (19) yielding static gain formulae (53) and (54) far more easily than by full p.d.e solution and setting p to zero subsequently. \underline{A}_o can be estimated even more simply from (18) and (19) by ignoring after transformation all but the p-dependent coefficients of the dependent variables giving

$$-p \underline{q} \approx \begin{pmatrix} -\epsilon & , & 0 \\ 0 & , & \alpha+1 \end{pmatrix} \underline{u} \quad \text{and hence } \underline{A}_o \approx \begin{pmatrix} \epsilon^{-1} & , & 0 \\ 0 & , & -(\alpha+1)^{-1} \end{pmatrix} \quad (65)$$

which agrees closely with the more accurate form

$$\underline{A}_o = \begin{pmatrix} (1+\alpha)\epsilon^{-1}/2 & , & 0 \\ 0 & , & -\alpha(\alpha+1)^{-1} \end{pmatrix} \quad (66)$$

derived from the full solution for $\underline{G}(o,p)$ via equation (60)

The straight vertical loci thus obtained for the elements $g_{A11}^{-1}(o,j\omega)$ and $g_{A22}^{-1}(o,j\omega)$ of $\underline{G}_A^{-1}(o,j\omega)$ are shown alongside the corresponding elements of $\underline{G}^{-1}(o,j\omega)$ in Figs. 4 and 5. The agreement for controller design is clearly more than adequate over the very wide frequency range considered

Unfortunately, for packed-columns such approximants are revealed in the companion paper to be far from adequate in some important situations.

It is interesting that \underline{A}_0 unlike \underline{A}_1 has not required use of the boundary conditions for its approximate determination above. This indicates that boundary conditions affect only the low frequency behaviour of the system, in accordance with our observations and deductions concerning the effect of terminal capacitance in Section 5.2.

Controllers designed on the basis of the m.v. 1st-order lag derived from simulated asymmetric, tray-column step responses have been successfully tested in simulation by Edwards and Owens⁽¹⁵⁾ for gains which increase the speed of response by up to five or six times.

7. Correlation with pilot plant data

Although the paper is intended primarily as a theoretical contribution, brief mention of a preliminary correlation of the model's predictions with experimental data would seem appropriate. Step-tests carried out on the 7m, 15 kw, 12-tray, water-ethanol pilot column at Sheffield produced the composition changes, shown in Fig. 9, measured on trays 1 and 10 with a liquid feed $F = 8.8$ mole/min @ $Z = 0.16$ into tray 6. The vapour rate changes from 5.0 to 8.0 mole/min at a constant reflux ratio of 2:1 making $v = 3.0$ and $l = 2.0$. Steady-state output compositions of 0.52 and 0.08 yield an average figure for 2GL of 0.44 and hence $G = 0.0367$, from which an effective value of $\epsilon = 1.88$ ($\alpha = 2.88$) is obtained via equation (30). (This suggests an effective relative volatility of about 4.0 which produces an ideal equilibrium curve coarsely approximating the true ethanol/water curve). Now for $v = 3$, $l = 2$ we deduce from our linearised model that

$$y = \{- |g_{22}| + 5 |g_{11}| \} G / 2V$$

and

$$x' = \{- |g_{22}| - 5 |g_{11}| \} G / 2V$$

and calculating the steady-state gains from (53) and (54), therefore predicts $y \approx$ zero (the g_{22} and g_{11} contributions nearly cancelling one another) and $x = -0.069$: in remarkably close accordance with the measured change.

The pilot column has large terminal capacitances of some 330 moles yielding a non-normalised value for $T' = 62$ mins. Now where end-capacitances dominate it is readily shown from (51) and (52) that

$$\lim_{L^{-1} \gg p \gg T^{-1}} \{p g_{11}(o,p)\} = \frac{\epsilon L}{2T} \quad \text{and} \quad \lim_{L^{-1} \gg p \gg T^{-1}} \{p' g_{22}(o,p)\} = - \frac{(\alpha+1)L}{T}$$

and from this latter formula and the static gain $g_{22}(o,o)$, a time constant of 42 min is predicted for the x' response. The predicted near-exponential response for x' shown in Fig. 9 is clearly most encouraging as is the very small deviation of the y -trace, in accord with prediction. The transient initial reversal of this trace is not unreasonable since, in the near counter-balance situation between the effects of g_{11} and g_{22} , it is quite possible, with slight parameter-change, for the high-frequency response to differ in sign to that of the ultimate response.

Clearly a large programme of trials is necessary, involving parameter variations as well as input-change, to validate all the many predictions from the parametric model. The experimental findings given are an encouraging beginning to this exercise, particularly in view of the wide departures from the symmetry and the small signal assumptions made in the model derivation.

8. Conclusions

It has proved possible to derive completely analytically and precisely, a transfer-function matrix relating composition changes y and x' at the column output to changes v and l in internal vapour and liquid flow-rate. The model parameters are readily related to plant parameters and nominal operating conditions. Its intended purpose is for controller design but

permitting a closer dialogue between control system designer and plant designer at an early stage in a project. The model is derived from initial assumptions frequently made in earlier dynamics studies either explicitly or implicitly, these being a piecewise linear equilibrium curve, spatially independent internal flow rates, constant tray loading, zero vapour capacitance and trays operating in equilibrium. Hydrodynamic effects on tray holdup are largely eliminated by concentrating on perturbations about the steady-state. (Previous researchers^(7,12) have in any event shown shown little loop interaction between composition dynamics and hydrodynamics which may therefore be treated separately).

The additional starting assumption is that of symmetry between rectifier and stripping section and a 50/50 feed-mixture, leading to nominally equal take-off rates of top and bottom product. The model is thus derived for a special case believed to be particularly relevant for twin product control, the symmetry leading to ready diagonalisation of the system matrices and comparative ease of solution. The model should, however, be sufficiently robust to apply, as a good approximation, to situations deviating from symmetry to a reasonable degree and a preliminary experimental test has confirmed this claim.

The model predicts the T.F.M. between $[\bar{y} - x', \bar{y} + x']^T$ and $[\bar{v} + \ell, \bar{v} - \ell]^T$ to be completely diagonal. The individual transfer-functions are shown to approximate first-order lag behaviour over a wide frequency range for long columns and a rapid method for determining such approximants has been demonstrated. These findings are in general accord with earlier research^(3,4,7,8,9,10,11,12) More complex behaviour at very high frequency is, however, predicted. In a companion paper on packed columns⁽¹⁾ it is shown that first-order lag behaviour it is not always a safe assumption however. Terminal capacitance is proved to affect only the low-frequency end of the system's frequency response.

Many more predicted effects of parameter variation may be made using the model and naturally this suggests a wide range of tests for its complete practical validation. Being a parametric model however, this makes the task of planning a full exploration of parameter space (including operating conditions) a much more systematic exercise.

9. References

- (1) Edwards, J.B. and Guilandoust, M. 'Parametric transfer-functions for packed, binary distillation columns', Trans. Inst. Chem. Engrs.
- (2) Judson King, C. 'Separation Processes' McGraw Hill, New York, 1971.
- (3) Wilkinson, W.L. and Armstrong, W.D., Chem.Eng.,Sci., 1957, 7(1/2).
- (4) Stainthorp, F.P. and Searson, H.M., Trans. Inst. Chem. Engrs., 1973, 51, 42.
- (5) Jawson, M.A. and Smith, W., 'Counter current transfer processes in non-steady state', Proc. Royal Soc., (London), A225, p. 226, 1965.
- (6) Voetter, H., 'Plant and process dynamic characteristics', Butterworth's Scientific Publications, 1957.
- (7) Rosenbrock, H.H. and Storey, C., 'Computational techniques for chemical engineers', Pergammon Press, 1966.
- (8) Kim, C. and Friedly, J.C., 'Approximate dynamic modelling of large staged systems', Ind. Eng., Chem., Process Des. Develop., Vol. 13, No. 2, p. 177, 1974.
- (9) Edwards, J.B. and Jassim, H.J. 'An analytical study of the dynamics of binary distillation columns', Trans. Inst. Chem., Engrs., 1977, 55, pp. 17-29.
- (10) Shinskey, F.G., 'Process control systems' 1967, (New York: McGraw-Hill).
- (11) McMorran, P.D., 'Application of the inverse Nyquist method to a distillation column model', Proc. of 4th U.K.A.C. Control Convention, 1971, p. 122.

- (12) Armstrong, W.D. and Wood, R.M. 'An introduction to the theoretical evaluation of the frequency response of a distillation column to a change in reflux flow rate', Trans. Instn. Chem. Engrs., Vol. 39, 1961, pp. 80-85.
- (13) Rademaker, O., Rijnsdorp, J.E. and Maarleveld, A., 'Dynamics and control of continuous distillation units', Elsevier, Amsterdam, 1975.
- (14) Owens, D.H. 'First and second-order-like structures in linear multivariable control system design', Proc. I.E.E., 1975, 122, (9), pp. 935-941.
- (15) Edwards, J.B. and Owens, D.H., 'First-order type models for multivariable process control', Proc. I.E.E., 1977, 124, (11), pp. 1083-1088.

Fig. 1 Vapour/liquid equilibrium curve and its piecewise linear approximation

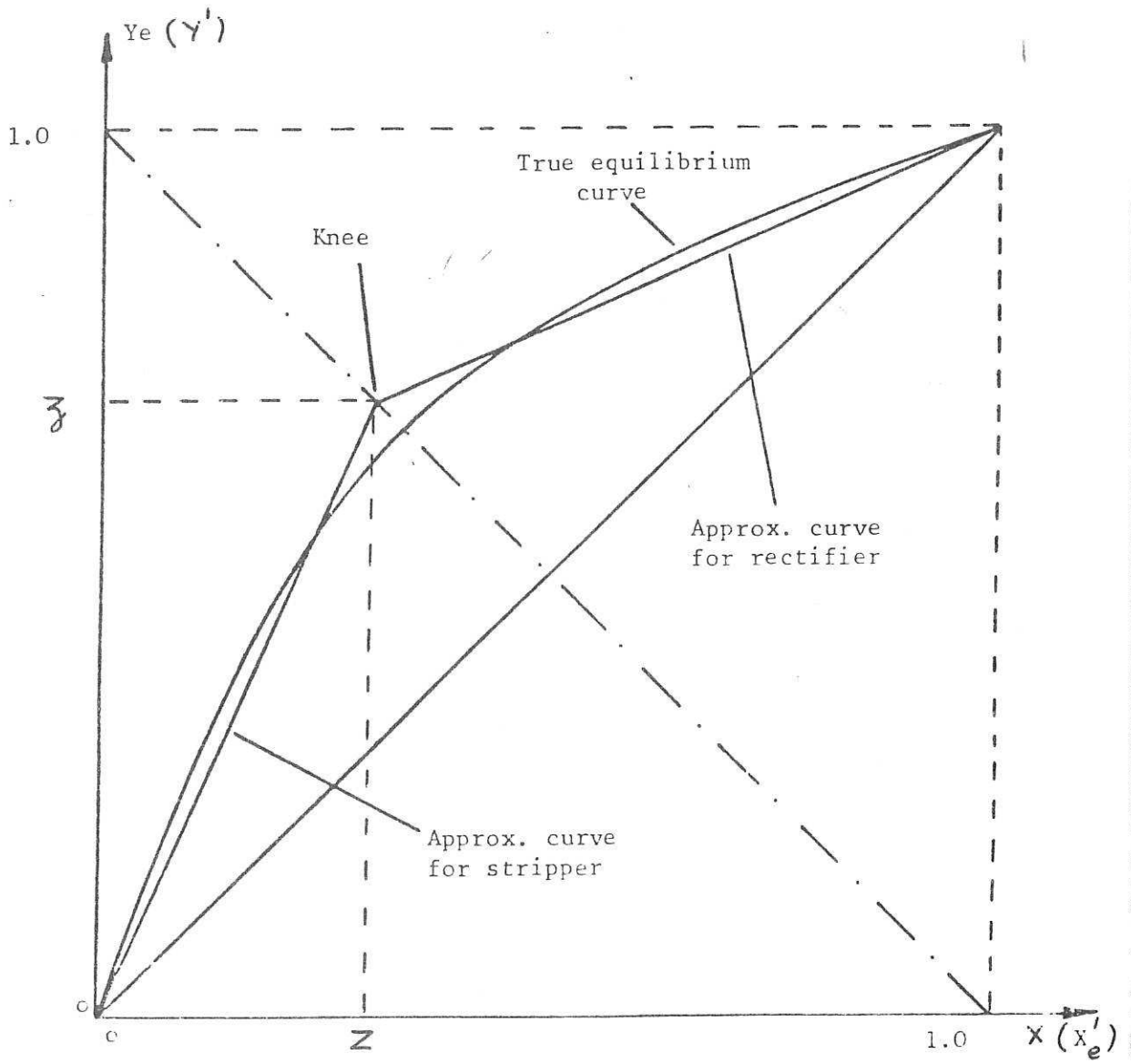
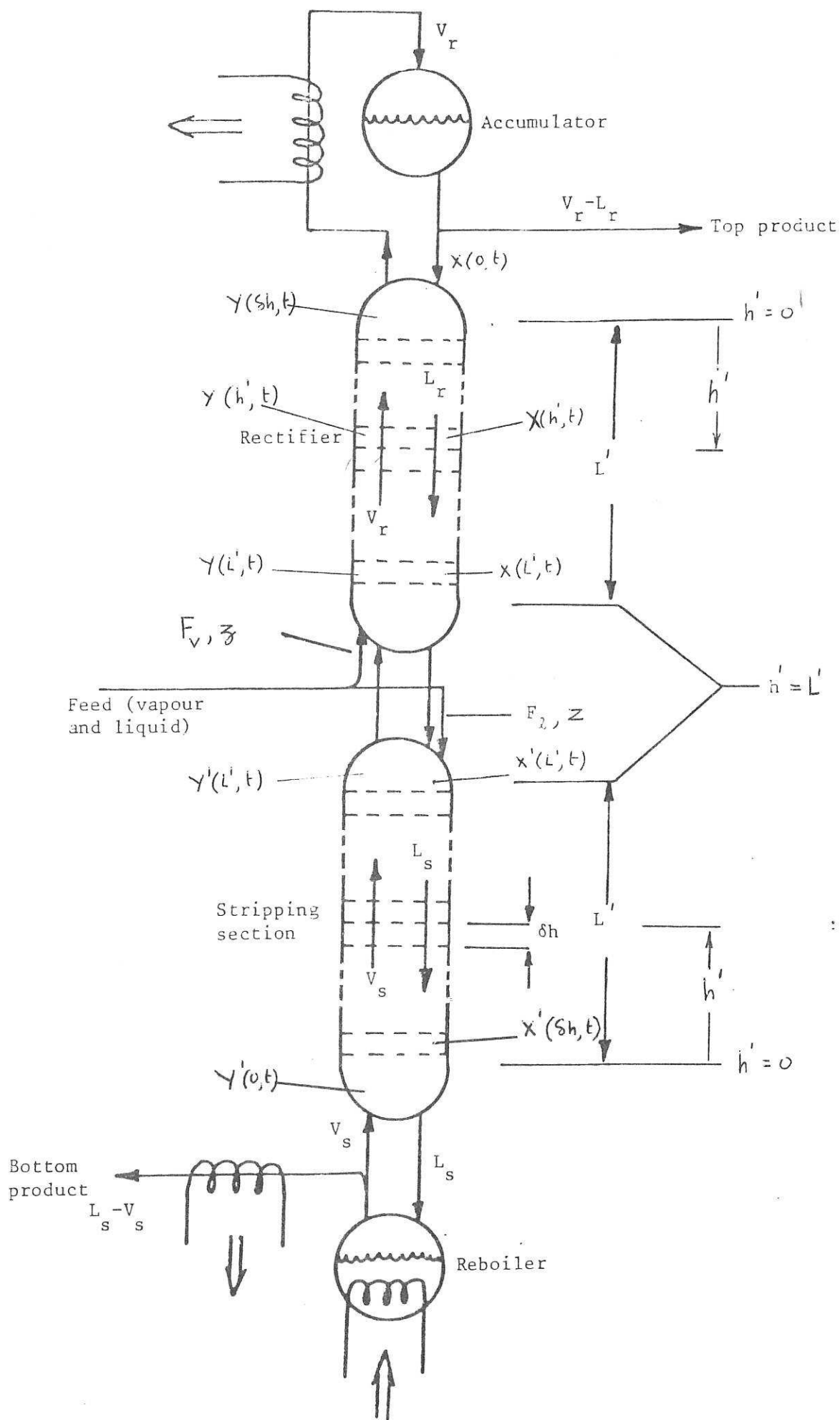


Fig. 2. Illustrating the Complete System



(4)

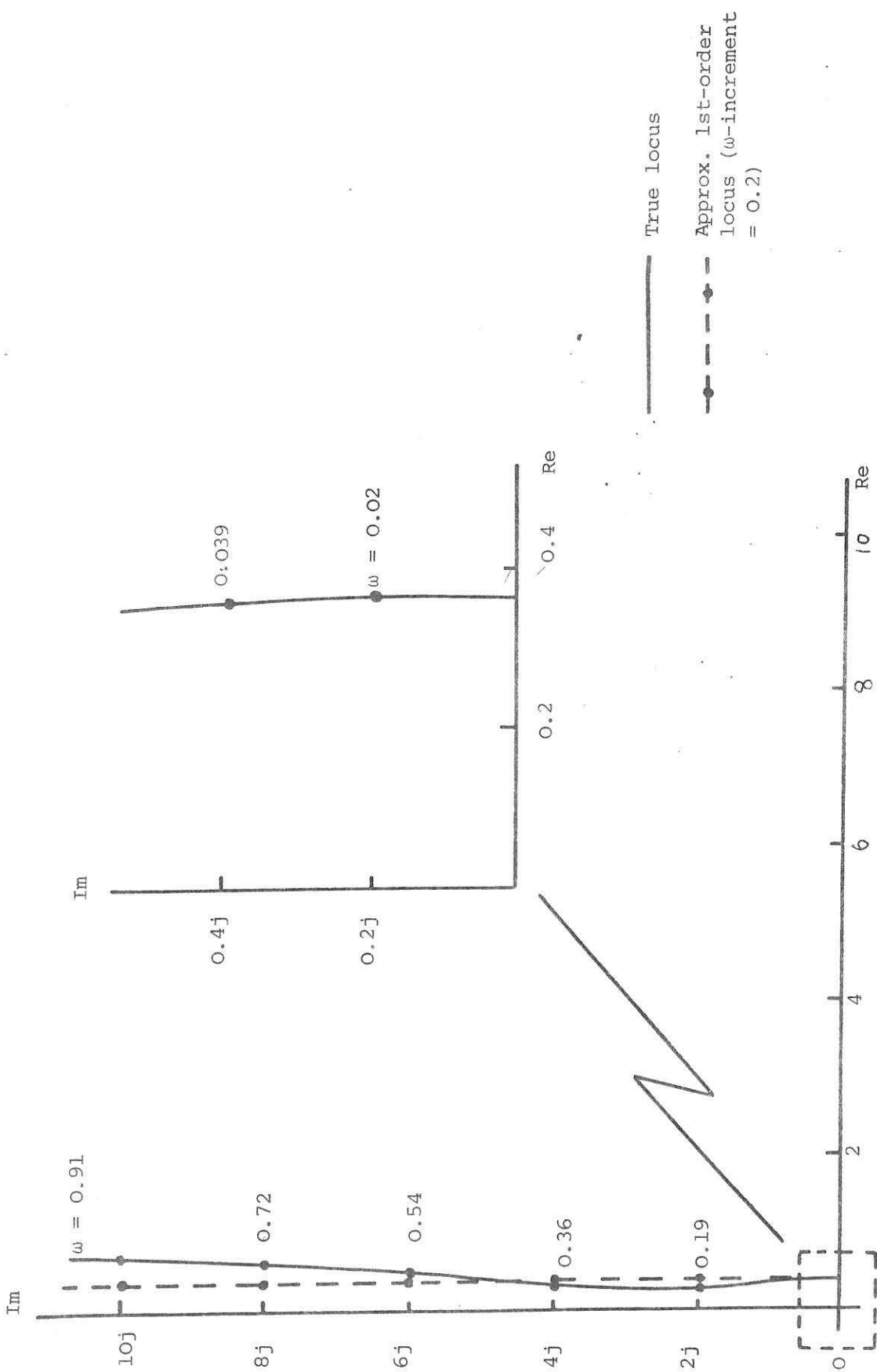


Fig. 4 Comparing accurate and 1-st order-lag model loci for $g_{11}^{-1}(s, j\omega)$

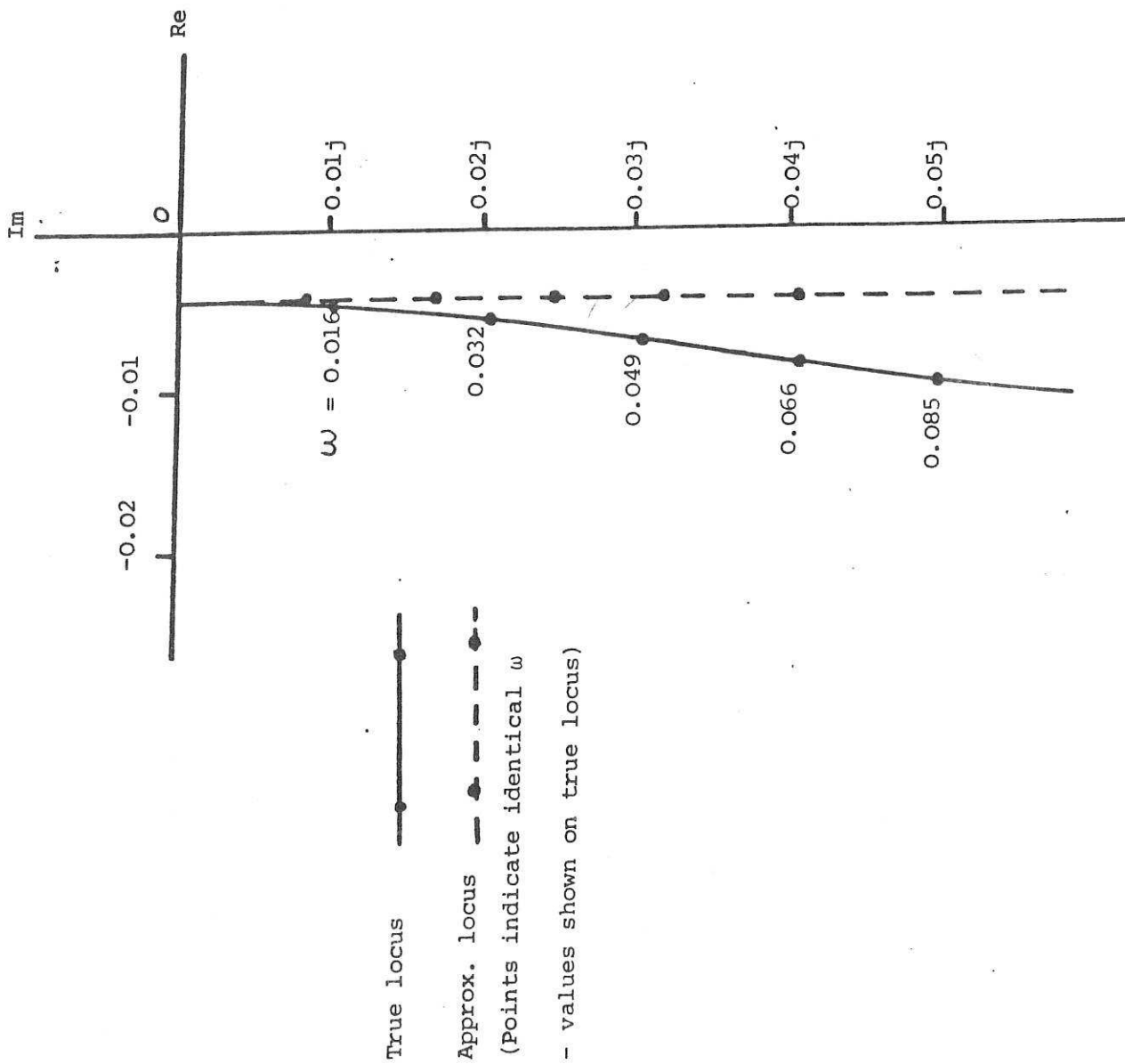


Fig. 5. Comparing accurate and 1-st order lag model loci for $\bar{g}_{2g}(0, j\omega)$

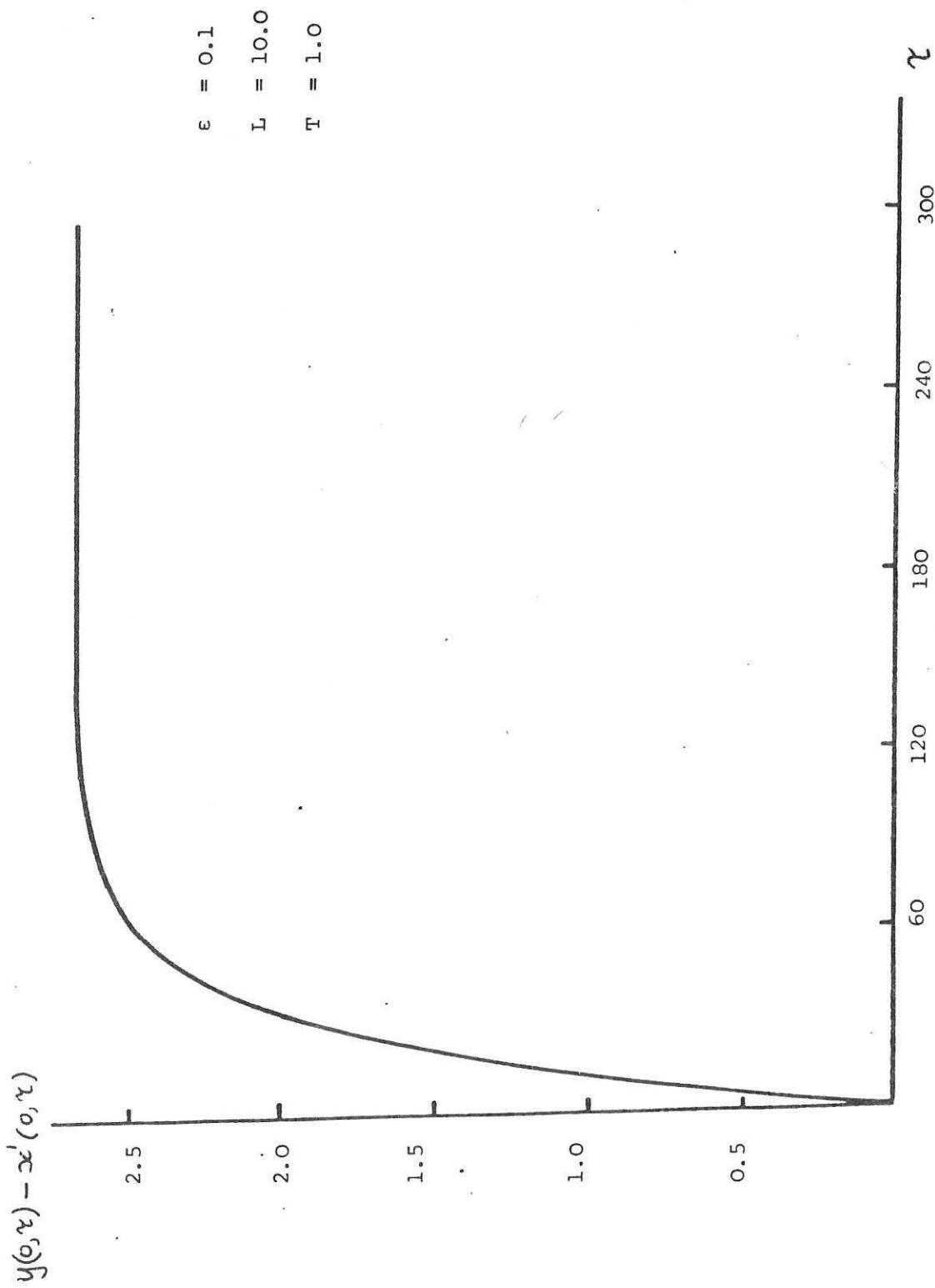


Fig. 6 Unit Step Response of $q_1(O,p)$

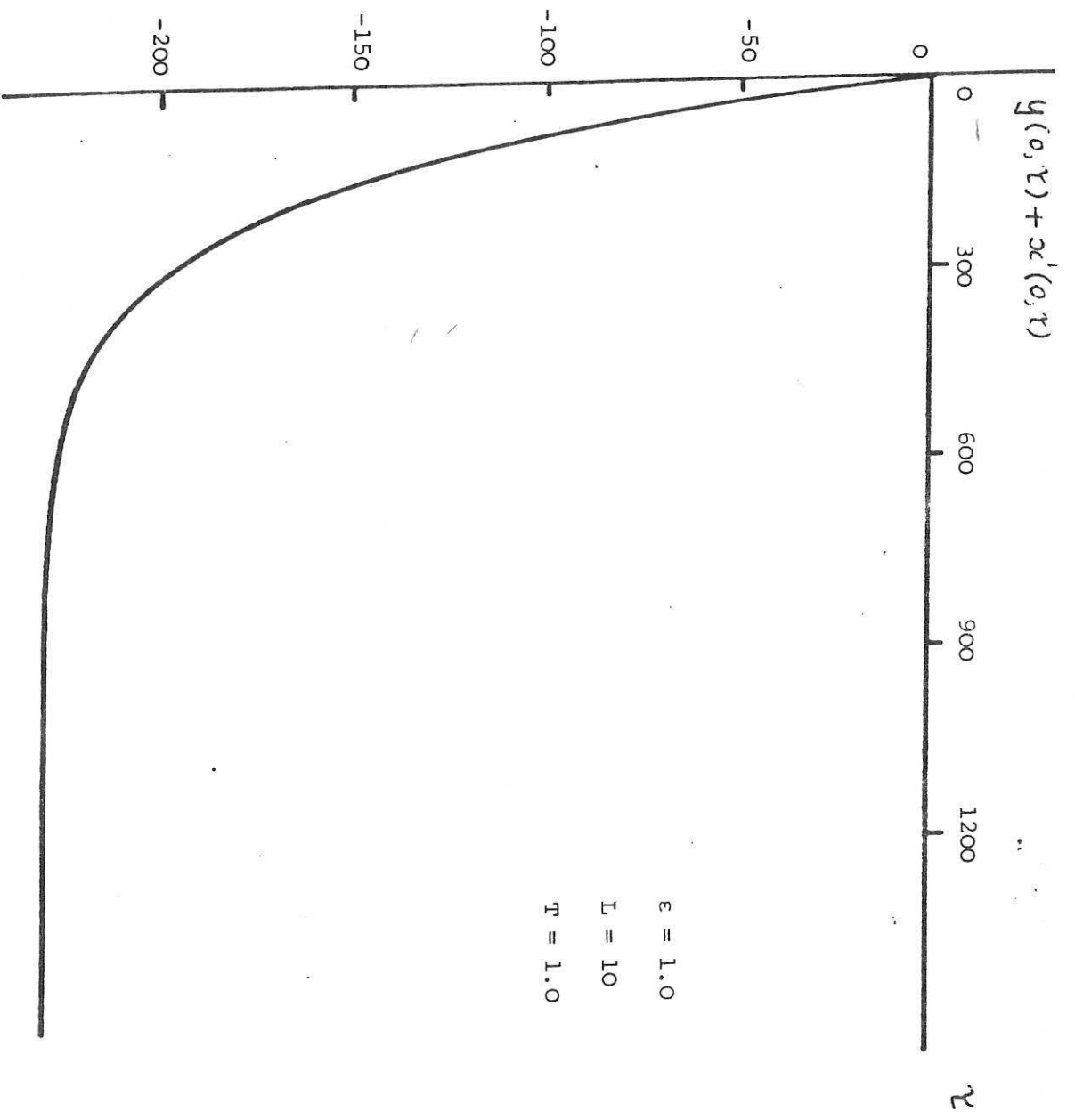


Fig. 7 Unit Step-response of $g_{22}(O,P)$

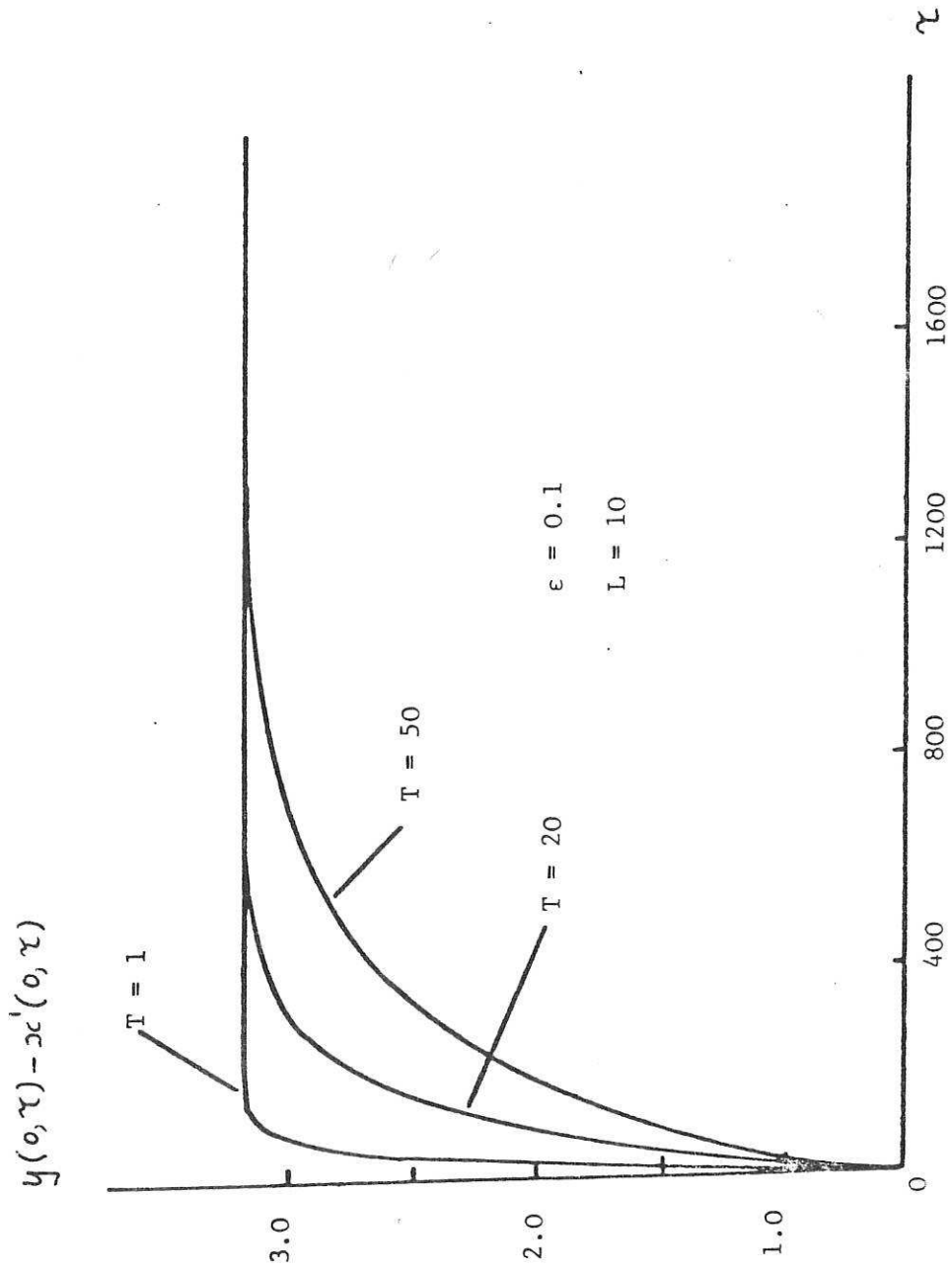


Fig. 8. Effect of terminal capacitance variation on unit step-response of $\bar{g}_{11}(0, p)$